

Supporting information for :
X-ray Crystallographic Structure of a Teixobactin Derivative
Reveals Amyloid-Like Assembly

Hyunjun Yang, Michał Wierzbicki, Derek R. Du Bois, and James S. Nowick*
Email: jsnowick@uci.edu

Department of Chemistry, University of California, Irvine,
Irvine, California 92697-2025, USA

Table of contents

Supplemental figures and table	S2
Table S1. MIC values of teixobactin analogues 2 and 3 .	
Figure S1. Solubility assays of teixobactin analogues 2 and 3 .	
Figure S2. Overlay of 32 independent molecules of teixobactin analogue 3 .	
Figure S3. Wall-eye stereo view of the dimer formed by teixobactin analogue 3 .	
Figure S4. Wall-eye stereo view of the double helix of β -sheet fibrils formed by teixobactin analogue 3 .	
Figure S5. Double helix of β -sheet fibrils formed by teixobactin analogue 3 illustrating the central cavity.	
Figure S6. Ramachandran plot of teixobactin analogue 3 .	
Materials and methods	
General information	S5
Synthesis of teixobactin analogues	S5
Minimum inhibitory concentration (MIC) assay of teixobactin analogues	S6
Solubility assay	S6
Thioflavin T (ThT) fluorescence assay	S6
Transmission electron microscopy (TEM) imaging	S7
Crystallization of <i>N</i> -Me-D-Phe ¹ , <i>N</i> -Me-D-Gln ₄ ,Lys ₁₀ -teixobactin (3)	S8
X-ray crystallographic data collection, data processing, and structure determination	S9
Table S2. Crystal data and structure refinement.	S10
Synthesis of Boc- <i>N</i> -Me-D-Phe ¹ -OH from D-phenylalanine	S11
¹ H NMR spectrum of Boc- <i>N</i> -Me-D-Phe ¹ -OH	S14
HPLC trace and mass spectrum of <i>N</i> -Me-D-Phe ¹ , <i>N</i> -Me-D-Gln ₄ ,Lys ₁₀ -teixobactin (3)	S15
References	S16

Supplemental figures and table

Table S1. MIC values of teixobactin analogues in $\mu\text{g/mL}$.

	<i>Staphylococcus aureus</i> ATCC 29213	<i>Staphylococcus epidermidis</i> ATCC 14990	<i>Bacillus subtilis</i> ATCC 6051	<i>Escherichia coli</i> ATCC 10798
Lys ₁₀ -teixobactin (2) ^a	1	0.5	1	>32
<i>N</i> -Me-D-Phe ^I ₁ , <i>N</i> -Me-D-Gln ₄ ,Lys ₁₀ -teixobactin (3) ^a	16	16	8	>32

^a Trifluoroacetic acid (TFA) salts.

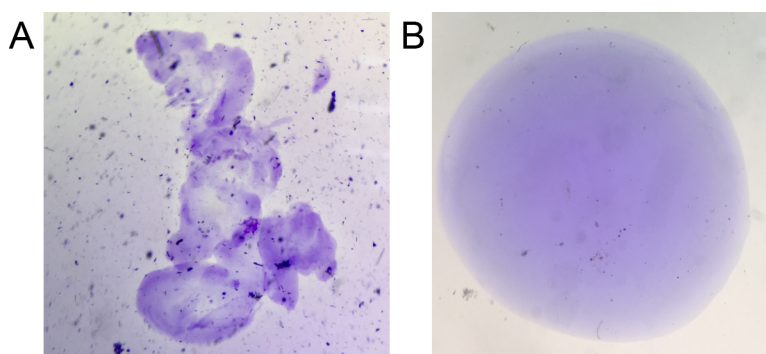


Figure S1. Solubility assays of (A) Lys₁₀-teixobactin (**2**) and (B) *N*-Me-D-Phe^I₁,*N*-Me-D-Gln₄,Lys₁₀-teixobactin (**3**). 1 μL of 20 mg/mL solution of peptide in DMSO was added to 20 μL of PBS buffer at pH 7.4 containing a small amount of crystal violet to aid in visualization.

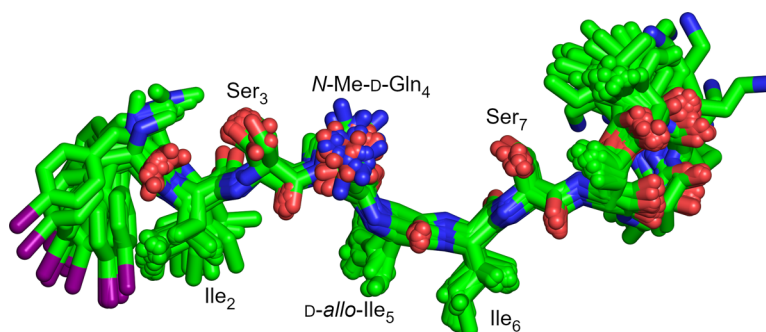


Figure S2. Overlay of the 32 crystallographically independent molecules of *N*-Me-D-Phe^I₁,*N*-Me-D-Gln₄,Lys₁₀-teixobactin (**3**).

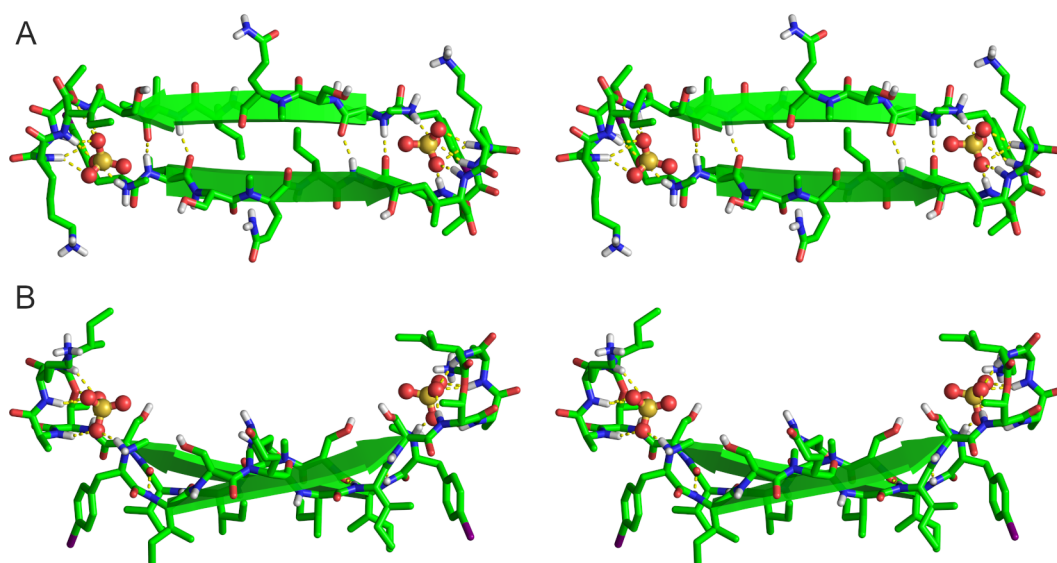


Figure S3. Wall-eye stereo view of the X-ray crystallographic structure of a representative dimer of *N*-Me-D-Phe^I₁,*N*-Me-D-Gln₄,Lys₁₀-teixobactin (**3**). (A) Top view. (B) Side view.

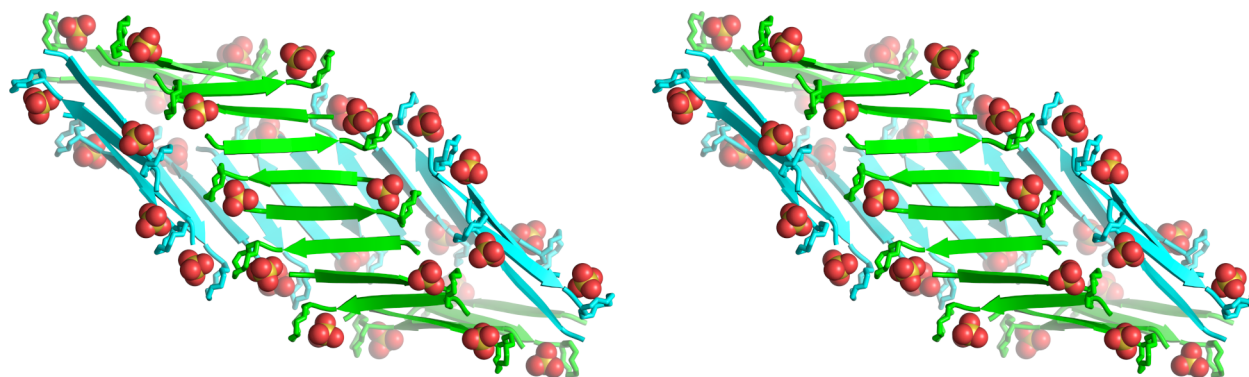


Figure S4. Wall-eye stereo view of the double helix of β -sheet fibrils formed by *N*-Me-D-Phe^I₁,*N*-Me-D-Gln₄,Lys₁₀-teixobactin (**3**). Sulfate anions are shown as spheres.

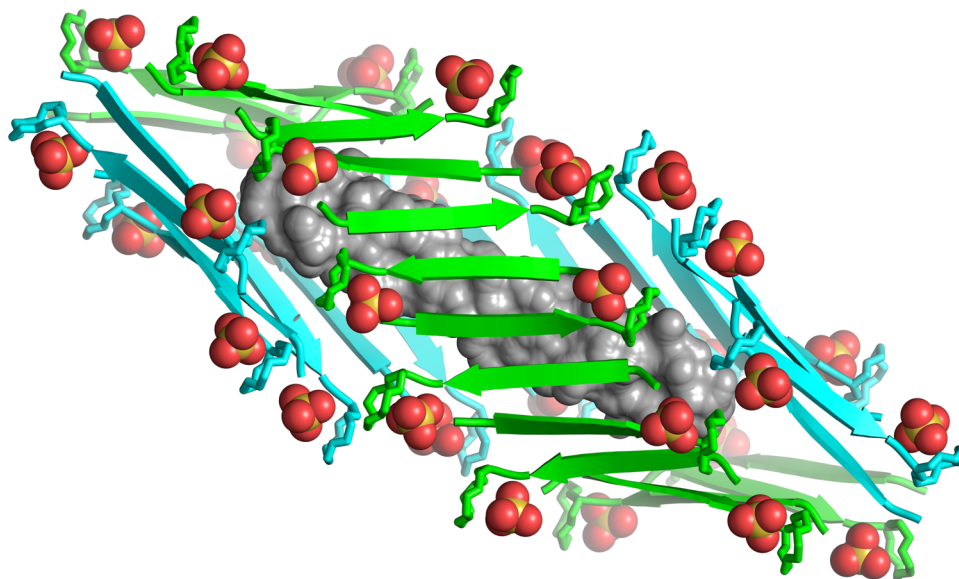


Figure S5. Double helix of β -sheet fibrils formed by N -Me-D-Phe^I₁, N -Me-D-Gln₄,Lys₁₀-teixobactin (**3**) illustrating the central cavity (grey surface).

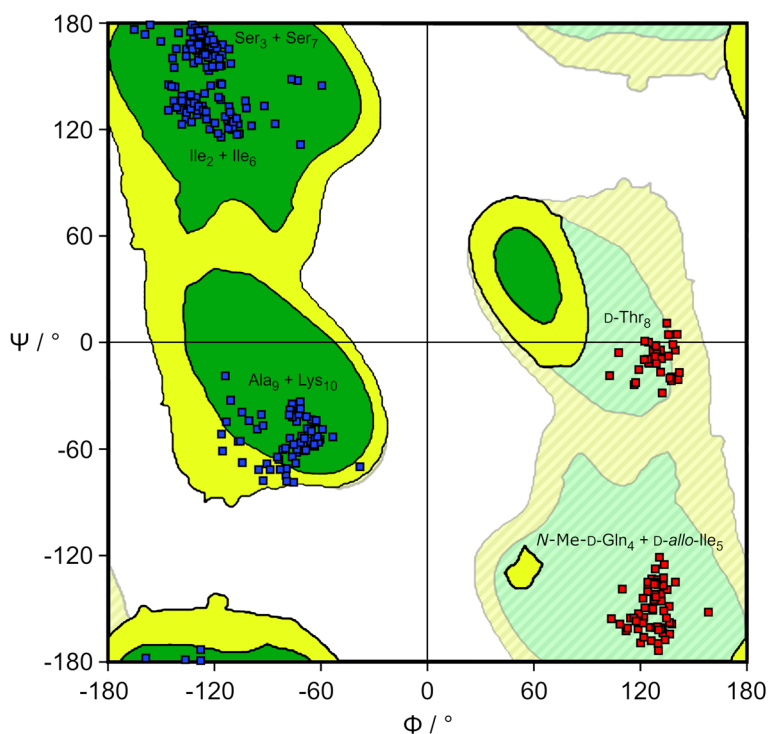


Figure S6. Ramachandran plot illustrating the ϕ and ψ angles of residues 2–10 of the 32 independent molecules of N -Me-D-Phe^I₁, N -Me-D-Gln₄,Lys₁₀-teixobactin (**3**). The dark green regions correspond to preferred dihedral angles for L-peptides and proteins; the yellow-green regions correspond to allowed regions for L-peptides and proteins; the pale green and yellow regions correspond to preferred and allowed dihedral angles for D-peptides and proteins.

Materials and Methods

General information

Methylene chloride (CH₂Cl₂) was passed through alumina under argon prior to use. Amine-free *N,N*-dimethylformamide (DMF) was purchased from Alfa Aesar. Fmoc-D-*allo*-Ile-OH was purchased from Santa Cruz Biotechnology. Fmoc-*N*-Me-D-Gln(Trt)-OH was purchased from Alabiochem Tech. Other protected amino acids were purchased from CHEM-IMPEX. Preparative reverse-phase HPLC was performed on a Rainin Dynamax instrument equipped with an Agilent Zorbax SB-C18 column. Analytical reverse-phase HPLC was performed on an Agilent 1260 Infinity II instrument equipped with a Phenomenex Aeris PEPTIDE 2.6 μ XB-C18 column. HPLC grade acetonitrile (MeCN) and deionized water (18 M Ω) containing 0.1% trifluoroacetic acid (TFA) were used as solvents for both preparative and analytical reverse-phase HPLC. Deionized water (18 M Ω) was obtained from a Barnstead NANOpure Diamond water purification system. Teixobactin analogues **2** and **3** were prepared and studied as the trifluoroacetate salts.

Synthesis of Lys₁₀-teixobactin (**2**) and *N*-Me-D-Phe^I₁,*N*-Me-D-Gln₄,Lys₁₀-teixobactin (**3**)

Lys₁₀-teixobactin (**2**) and *N*-Me-D-Phe^I₁,*N*-Me-D-Gln₄,Lys₁₀-teixobactin (**3**) were synthesized as the trifluoroacetate salts using procedures we have previously reported.¹ Dry DMF was used instead of a mixture of MeCN/THF/CH₂Cl₂ for the cyclization step. In the synthesis of *N*-Me-D-Phe^I₁,*N*-Me-D-Gln₄,Lys₁₀-teixobactin (**3**), Boc-*N*-Me-D-Phe^I₁-OH was used instead of Boc-*N*-Me-D-Phe₁-OH. Coupling of Fmoc-Ser₃(tBu)-OH after *N*-Me-D-Gln₄ was performed using 4 equiv Fmoc-Ser₃(tBu)-OH with coupling reagent HATU (4 equiv), HOAt (4 equiv) in 20% (v/v) collidine in dry DMF (5 mL) for 12 h.

Minimum inhibitory concentration (MIC) assay of teixobactin analogues

MIC assays of teixobactin analogues **2** and **3** were performed using procedures we have previously reported.¹

Solubility assay

Solubility assays of teixobactin analogues **2** and **3** were performed using procedures we have previously reported.²

Thioflavin T (ThT) fluorescence assay

Preparation of buffered ThT solution. The ThT solution was freshly prepared before use. A solution of 20 μM ThT was prepared in a 1x PBS buffer at pH 7.4 (5 mL). The solution was filtered through a 0.2-micron syringe filter. The concentration of ThT in the solution was determined using a UV-vis spectrophotometer ($\epsilon = 36000 \text{ M}^{-1} \text{ cm}^{-1}$ at 412 nm) and adjusted to 20 μM .

ThT fluorescence assay. ThT fluorescence assays were conducted in 96-well plates (96 Well Optical Bottom Black, Polymer base, NUNC, Rochester, NY, USA). A 200- μL aliquot of ThT solution in PBS (above) was transferred to each of four wells of 96-well plate. A 1.73- μL aliquot of a 20 mg/mL solution of Lys₁₀-teixobactin in DMSO was added to each well to give 119 μM Lys₁₀-teixobactin and 20 μM ThT in PBS. The 96-well plate was sealed with adhesive plate sealers. The plate was immediately inserted into a Varioskan LUX multimode microplate reader (Thermo Fisher Scientific) and incubated at 37°C while shaking (1200 rpm, high shaking force) and monitoring fluorescence (444 nm excitation, 480 nm emission, 12 nm slit width) every 20 min over 5 days using the bottom-read mode.

Transmission electron microscopy (TEM) imaging

Sample preparation. Lys₁₀-teixobactin in DMSO (10 mg/mL concentration) was diluted to 100 μ M with PBS buffer at pH 7.4. The solution was incubated at 37 °C over 72 h with shaking. A TEM grid (Formvar/carbon film on 400 mesh copper) was treated by glow discharge using a Leica EM ACE200 vacuum coater (Leica Microsystems, Buffalo Grove, IL, USA). A 5- μ L aliquot of the Lys₁₀-teixobactin solution was applied to the TEM grid. After 15 sec, the solution was wicked away with filter paper and the grid was immediately washed with two 200- μ L aliquots of distilled H₂O. The distilled H₂O was wicked away with filter paper and the grid was immediately stained with 2% uranyl acetate in H₂O (5 μ L) for 15 sec. The remaining solution was wicked away from the grid with filter paper.

TEM Imaging. TEM images of Lys₁₀-teixobactin were taken with a JEM-2100F transmission electron microscope (JEOL, Peabody, MA, USA) at 200 kV with an electron dose of approximately 15 e⁻/Å². The microscope was equipped with Gatan K2 Summit direct electron detector (Gatan, Pleasanton, CA, USA) at 15,000x or 25,000x magnification. The sample was cooled at liquid nitrogen temperature through the cryostage. Contrast and brightness of the images were adjusted as appropriate.

Crystallization of *N*-Me-D-Phe^I₁,*N*-Me-D-Gln₄,Lys₁₀-teixobactin (**3**)

N-Me-D-Phe^I₁,*N*-Me-D-Gln₄,Lys₁₀-teixobactin (**3**) was dissolved in 0.2 micron syringe filtered NANOpure H₂O (10 mg/mL). Crystallization conditions were screened by screening in a 96-well plate format using three crystallization kits from Hampton Research (PEG/Ion, Index, and Crystal Screen). Each well was loaded with 100 μ L of a different mother liquor solution from the kits. The hanging drops were set up using a TTP Labtech Mosquito[®] liquid handling instrument. Hanging drops were made by combining an appropriate volume of teixobactin analogue **3** with an appropriate volume of well solution to create three 150-nL hanging drops with 1:1, 1:2, and 2:1 peptide:well solution. Rectangular rod-shaped crystals grew in all conditions that contained sulfate salts (Li₂SO₄, MgSO₄, Na₂SO₄, K₂SO₄, (NH₄)₂SO₄) and polyethylene glycol (PEG) 3,350.

Crystal growth was optimized using conditions containing Na₂SO₄. In the optimization, the Na₂SO₄ and PEG 3,350 concentrations were varied across the 4x6 matrix of a Hampton VDX 24-well plate to afford crystals suitable for X-ray diffraction. The hanging drops for these optimizations were prepared on glass slides by combining 1 or 2 μ L of teixobactin solution with 1 or 2 μ L of well solution in ratios of 1:1, 2:1, and 1:2. Crystals that formed were checked for diffraction using a Rigaku Micromax-007 HF diffractometer with a Cu anode at 1.54 Å. Through these optimization studies the following conditions were selected: 0.19 M Na₂SO₄ and 15% PEG 3,350.* No cryoprotectant was used other than the PEG 3,350 already present in the drop.

* These conditions afforded multiple crystals that diffracted to 3 or 4 Å, but only one crystal that diffracted to 2 Å. All of the crystals had comparable unit cell dimensions, but the crystal for which the dataset (below) was collected gave the best diffraction data. After collecting data needed to obtain anomalous signal at 6 keV, the crystal had degraded to a point where it was no longer possible to collect adequate data at higher energy (ca. 12 keV).

X-ray crystallographic data collection, data processing, and structure determination

Data collection was performed with the Blu-Ice software³ at Stanford Synchrotron Radiation Lightsource using BL 9-2 beamline at a wavelength of 2.06633 Å. The rotation method was employed and four sets of 360 images each were collected at a 0.5° rotation interval (a total of two complete rotations). The four sets were processed separately with XDS⁴, and the resulting datasets were merged with BLEND⁵. The structure was solved with SAD phasing implemented in the Hybrid Substructure Search (HySS)⁶ module of the Phenix suite⁷. Iodine atoms of the *N*-Me-D-Phe^I₁ residues were used as sources of the anomalous signal. The initial electron density maps were generated using the substructure coordinates as initial positions in Autosol⁸. The structure was then refined with REFMAC5⁹ under CCP4¹⁰ using Coot¹¹ for model building. All B-factors were refined isotropically and riding hydrogen atoms coordinates were generated geometrically. The bond length, angles, and torsions restraints for unnatural amino acids (*N*-Me-D-Phe^I, *N*-Me-D-Gln, and *D-allo*-Ile) were generated with AceDRG¹² under CCP4.

Table S2. Crystallographic properties, crystallization conditions, data collection, and model refinement statistics for teixobactin analogue **3**

Teixobactin analogue 3	
PDB ID	6E00
space group	P2 ₁ 2 ₁ 2 ₁
<i>a</i> , <i>b</i> , <i>c</i> (Å)	47.5, 69.4, 115.4
α , β , γ (°)	90, 90, 90
peptides per asymmetric unit	32
crystallization conditions	0.19 M Na ₂ SO ₄ , 15% PEG 3,350
Data collection	
wavelength (Å)	2.06633
resolution (Å)	39.21 - 2.20 (2.279 - 2.200)
total reflections	479611 (24317)
unique reflections	17797 (1370)
Multiplicity	21.20 (15.1)
completeness (%)	93.36 (67.87)
mean I/ σ	8.8 (1.48)
<i>R</i> _{merge}	0.339 (1.314)
<i>R</i> _{measure}	0.348 (1.36)
CC _{1/2}	0.991 (0.467)
CC*	0.998 (0.798)
Refinement	
<i>R</i> _{work}	0.211 (0.216)
<i>R</i> _{free}	0.246 (0.294)
number of non-hydrogen atoms per ASU	3037
RMS _{bonds}	0.011
RMS _{angles}	1.880
Ramachandran	
favored (%)	100
outliers (%)	0
clashscore	6
average B-factor	20.2

Synthesis of Boc-*N*-Me-D-Phe^I-OH from D-phenylalanine (D-Phe-OH)

Boc-*N*-Me-D-Phe^I-OH was synthesized from D-Phe-OH in the following steps: first to Boc-D-Phe^I-OH following Richardson et al. *J. Org. Chem.* **2018**, 83, 4525-4536 and then to Boc-*N*-Me-D-Phe^I-OH following Malkov et al. *Tetrahedron* **2006**, 62, 264-284.^{13,14} The yields were not optimized as the products were synthesized and used from the first batch of synthesis.

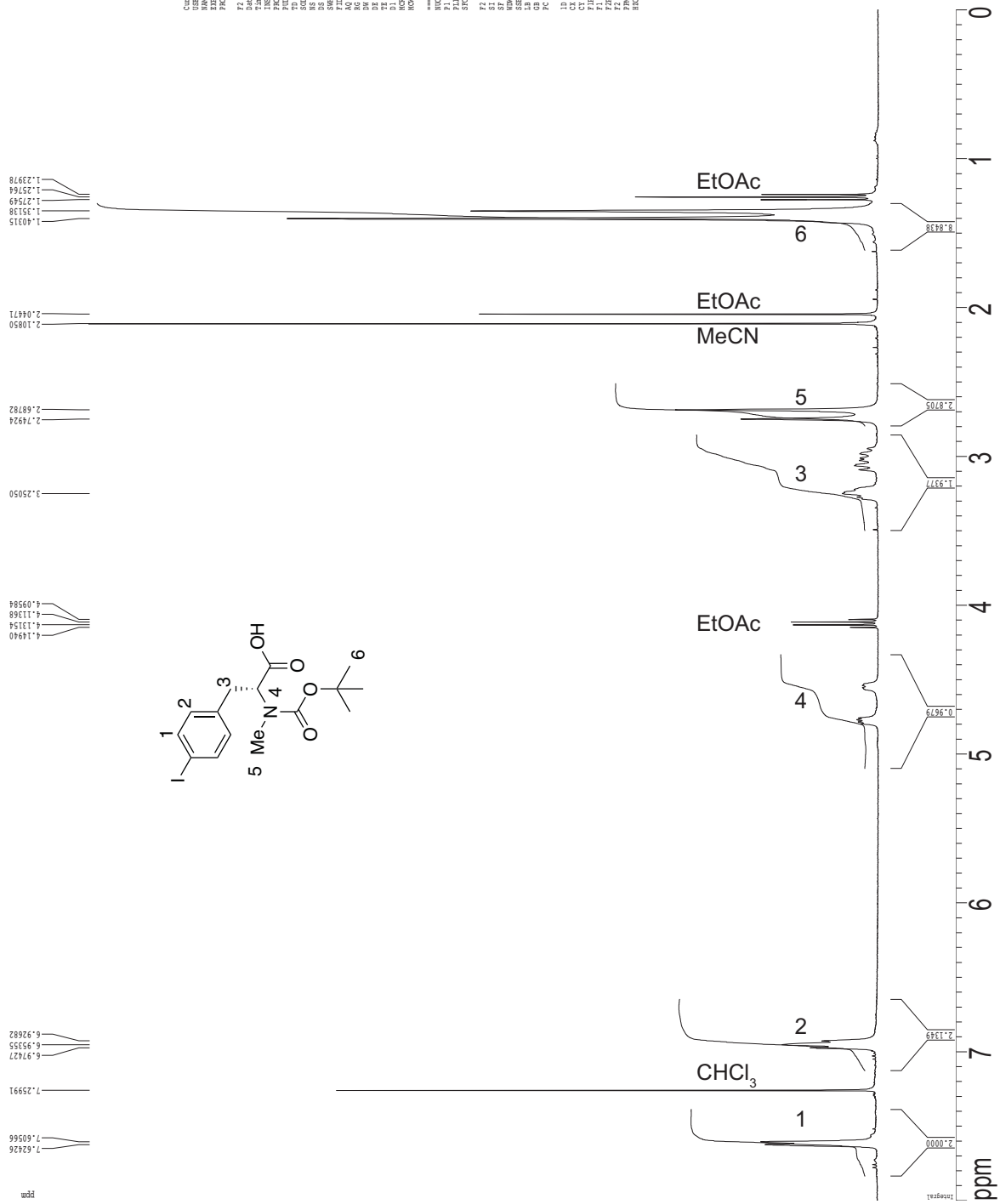
D-Phe^I-OH.¹³ D-Phenylalanine (3.0 g, 18.2 mmol), NaIO₃ (0.82 g, 7.26 mmol), and I₂ (1.84 g, 7.26 mmol) were dissolved in a mixture of 18.2 mL glacial acetic acid and 2.18 mL concentrated H₂SO₄. The mixture was heated to 70 °C and stirred under nitrogen for 24 h. NaIO₄ (116.6 mg, 0.544 mmol) was added and the mixture was heated to 70 °C with stirring under nitrogen for 24 h. The mixture was concentrated by rotary evaporator to ca. 15 mL. The residue was dissolved with H₂O (50 mL) and transferred to a separatory funnel. The mixture was washed with Et₂O (2 x 50 mL) and then with CH₂Cl₂ (50 mL). The aqueous phase was transferred to an Erlenmeyer flask and cooled to 0 °C on an ice bath. The pH was adjusted to 7.0 by slowly adding 5 M aq KOH with stirring (ca. 25 mL of 5 M aq KOH was used). A white solid precipitated and was isolated by filtration with a Büchner funnel. The solid was transferred to an Erlenmeyer flask and dissolved in 50% EtOH solution (20 mL). The mixture was heated to 85 °C in an oil bath. 20-mL aliquots of boiling 50% EtOH were added repeatedly until a clear yellow solution was obtained. (ca. 125 mL of boiling 50% EtOH was used). The hot solution was filtered through glass wool and was left for 12 h at room temperature to achieve crystallization. The resulting crystals were collected by Büchner funnel filtration and was washed with 50 mL of ice cold 50% EtOH solution. The solid was placed under vacuum (\leq 100 mTorr) to remove any residual solvents. The yield of D-Phe^I-OH was 1.98 g (38% yield).

Boc-D-Phe^I-OH.¹³ D-Phe^I-OH (2.0 g, 6.9 mmol) and Boc₂O (2.4g, 11.0 mmol) were dissolved in a mixture of MeOH (3.5 mL), H₂O (3.5 mL), and Et₃N (2.4 mL). The mixture was heated to 55 °C under nitrogen with stirring for 16 h. The mixture was concentrated by rotary evaporator and the resulting residue was dried under vacuum (\leq 100 mTorr). The residue was dissolved in EtOAc (30 mL) and cooled to 0 °C on an ice bath. The mixture was added to a separatory funnel containing 250 mM aq HCl (50 mL) and shaken vigorously for 15 s. The organic phase was collected, and the pH of the aqueous phase was adjusted to pH 1 with 1 M aq HCl. The aqueous phase was extracted with EtOAc (2 x 20 mL) and then organic phases were combined, washed with 250 mM aq HCl in saturated aqueous NaCl solution (30 mL), dried with MgSO₄, then filtered through Celite. The filtrate was evaporated by rotary evaporator and the residue was dried under vacuum (\leq 100 mTorr) to give a white foam. The product was recrystallized by suspending in 30 mL of hot hexane with stirring and adding hot Et₂O in 2-mL aliquots until a clear yellow solution was obtained (ca. 60 mL Et₂O added). The solution was transferred to a beaker and boiled until the volume read ca. 30 mL. The product was crystallized by cooling the solution on an ice bath and isolated by filtration using a Büchner funnel. The crystals were washed with cold hexane. The yield of Boc-D-Phe^I-OH was 1.71 g (65% yield).

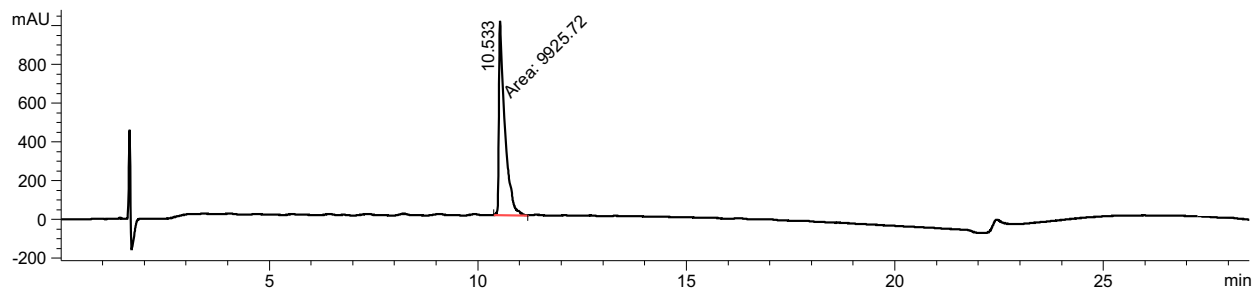
Boc-N-Me-D-Phe^I-OH.¹⁴ Boc-D-Phe^I-OH (1.71 g, 4.4 mmol) and MeI (2.74 mL, 44 mmol) were dissolved in THF (20 mL) at 0 °C and then NaH (60% dispersion in mineral oil, 1.76 g in oil, 44 mmol) was slowly added. The mixture was stirred at room temperature for 24 h under nitrogen. The mixture was quenched with H₂O (15 mL) and EtOAc (10 mL) was added. The solvents were evaporated by rotary evaporator and the residue was dried under vacuum (\leq 100 mTorr). The residue was dissolved in H₂O (300 mL) and transferred to a separatory funnel. The solution was washed with EtOAc (150 mL) and the aqueous solution was collected and acidified

to pH 3.5 with 5% citric acid. The suspension was extracted with EtOAc (200 mL) and the organic phase was washed with saturated aq NaCl (50 mL), H₂O (50 mL), and then dried with MgSO₄, and filtered through a Büchner funnel filtration. The resulting solution was evaporated by rotary evaporator and the residue was dried placed under vacuum (\leq 100 mTorr) to yield 0.78 g of Boc-*N*-Me-D-Phe^I-OH (44% yield). MS (negative ion mode) calcd for C₁₅H₁₉INO₄⁻ [M - H]⁻ m/z 404.04, found 404.88. Boc-*N*-Me-D-Phe^I-OH was used for solid-phase peptide synthesis without further purification.

¹H Spectrum of Boc-N-Me-D-Phe-OH



HPLC trace and mass spectrum of *N*-Me-D-Phe^I₁,*N*-Me-D-Gln₄,Lys₁₀-teixobactin (**3**)

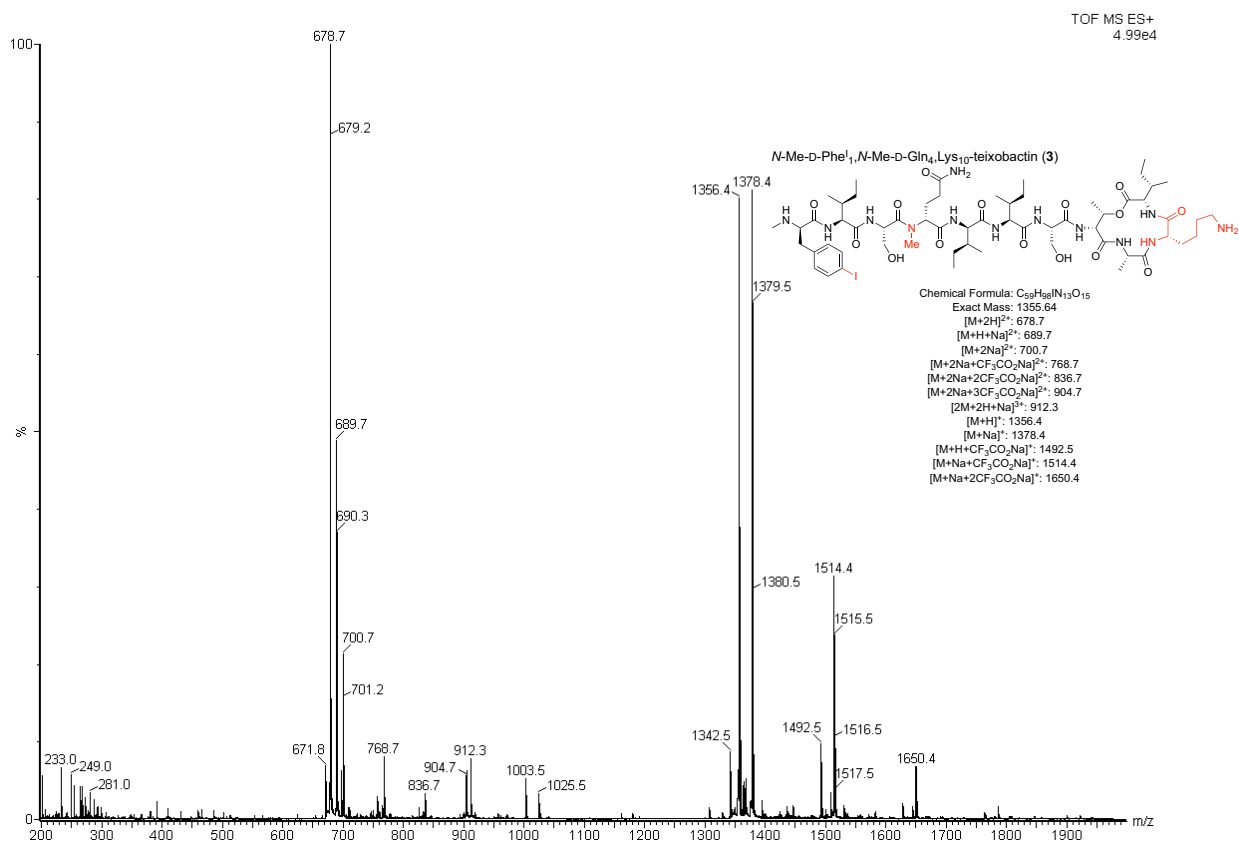


Area Percent Report

Sorted By : Signal
 Signal 1: MWD1 A, Sig=214,4 Ref=off
 Inj Volume : 20.000 µl

Peak #	RetTime [min]	Type	Width [min]	Area [mAU*s]	Height [mAU]	Area %
1	10.533	MM	0.1644	9925.71680	1006.51044	100.0000

Totals : 9925.71680 1006.51044



References

- 1 Yang, H.; Chen, K. H.; Nowick, J. S. *ACS Chem. Biol.* **2016**, *11*, 1823-1826.
- 2 Chen, K. H.; Le, S. P.; Han, X.; Fraix, J. M.; Nowick, J. S. *Chem. Commun.* **2017**, *53*, 11357-11359.
- 3 McPhillips, T. M.; McPhillips, S. E.; Chiu, H. J.; Cohen, A. E.; Deacon, A. M.; Ellis, P. J.; Garman, E.; Gonzalez, A.; Sauter, N. K.; Phizackerley, R. P.; Soltis, S. M.; Kuhn, P. J. *Synchrotron Rad.* **2002**, *9*, 401-406.
- 4 Kabsch, W. *Acta Crystallogr., Sect. D: Biol. Crystallogr.* **2010**, *66*, 125-132.
- 5 Foadi, J.; Aller, P.; Alguel, Y.; Cameron, A.; Axford, D.; Owen, R. L.; Armour, W.; Waterman, D. G.; Iwata, S.; Evans, G. *Acta Crystallogr., Sect. D: Biol. Crystallogr.* **2013**, *69*, 1617-1632.
- 6 Grosse-Kunstleve, R. W.; Adams, P. D. *Acta Crystallogr., Sect. D: Biol. Crystallogr.* **2003**, *59*, 1966-1973.
- 7 Adams, P. D.; Afonine, P. V.; Bunkoczi, G.; Chen, V. B.; Davis, I. W.; Echols, N.; Headd, J. J.; Hung, L. W.; Kapral, G. J.; Grosse-Kunstleve, R. W.; McCoy, A. J.; Moriarty, N. W.; Oeffner, R.; Read, R. J.; Richardson, D. C.; Richardson, J. S.; Terwilliger, T. C.; Zwart, P. H. *Acta Crystallogr., Sect. D: Biol. Crystallogr.* **2010**, *66*, 213-221.
- 8 Terwilliger, T. C.; Adams, P. D.; Read, R. J.; McCoy, A. J.; Moriarty, N. W.; Grosse-Kunstleve, R. W.; Afonine, P. V.; Zwart, P. H.; Hung, L. W. *Acta Crystallogr., Sect. D: Biol. Crystallogr.* **2009**, *65*, 582-601.
- 9 Murshudov, G. N.; Vagin, A. A.; Dodson, E. J. *Acta Crystallogr., Sect. D: Biol. Crystallogr.* **1997**, *53*, 240-255.
- 10 Winn, M. D.; Ballard, C. C.; Cowtan, K. D.; Dodson, E. J.; Emsley, P.; Evans, P. R.; Keegan, R. M.; Krissinel, E. B.; Leslie, A. G. W.; McCoy, A.; McNicholas, S. J.; Murshudov, G. N.; Pannu, N. S.; Potterton, E. A.; Powell, H. R.; Read, R. J.; Vagin, A.; Wilson, K. S. *Acta Crystallogr., Sect. D: Biol. Crystallogr.* **2011**, *67*, 235-242.
- 11 Emsley, P.; Lohkamp, B.; Scott, W. G.; Cowtan, K. *Acta Crystallogr., Sect. D: Biol. Crystallogr.* **2010**, *66*, 486-501.
- 12 Long, F.; Nicholls, R. A.; Emsley, P.; Gražulis, S.; Merkys, A.; Vaitkus, A.; Murshudov, G. N. *Acta Crystallogr., Sect. D: Biol. Crystallogr.* **2017**, *73*, 112-122.
- 13 Richardson, M. B.; Brown, D. B.; Vasquez, C. A.; Ziller, J. W.; Johnston, K. M.; Weiss, G. A. *J. Org. Chem.* **2018**, *83*, 4525-4536.
- 14 Malkov, A. V.; Stončius, S.; MacDougall, K. N.; Mariani, A.; McGeoch, G. D.; Kočovský, P. *Tetrahedron* **2006**, *62*, 264-284.